Influence of J series prostaglandins on apoptosis and tumorigenesis of breast cancer cells

Carl E.Clay[1], Andrew M.Namen[1], Gen-ichi Atsumi[1], Mark C.Willingham[2], Kevin P.High[1], Timothy E.Kute[2], Anthony J.Trimboli[1], Alfred N.Fonteh[1], Paul A.Dawson[1] and Floyd H.Chilton[1,3,4]

[1]Department of Internal Medicine, [2]Department of Pathology and [3]Department of Physiology and Pharmacology, Wake Forest University School of Medicine, Medical Center Boulevard, Winston Salem, NC 27157-1054, USA

[4]To whom correspondence should be addressed
Email: fchilton@wfubmc.edu

This study was undertaken to investigate the influence of the peroxisome proliferator-activated receptor γ (PPARγ) agonists on the proliferation, apoptosis and tumorigenesis of breast cancer cells. PPARγ investigation has been largely restricted to adipose tissue, where it plays a key role in differentiation, but recent data reveal that PPARγ is expressed in several transformed cells. However, the function of PPARγ activation in neoplastic cells is unclear. Activation of PPARγ with the known prostanoid agonist 15-deoxy-Δ12,14-prostaglandin J_2 (15dPGJ$_2$) or the thiazolidinedione (TZD) agonist troglitazone (TGZ) attenuated cellular proliferation of the estrogen receptor-negative breast cancer cell line MDA-MB-231, as well as the estrogen receptor-positive breast cancer cell line MCF-7. This was marked by a decrease in total cell number and by an inhibition of cell cycle progression. Addition of 15dPGJ$_2$ was not associated with an increase in cellular differentiation, as has been seen in other neoplastic cells, but rather induction of cellular events associated with programmed cell death, apoptosis. Video time-lapse microscopy revealed that 15dPGJ$_2$ induced morphological changes associated with apoptosis, including cellular rounding, blebbing, the production of echinoid spikes, blistering and cell lysis. In contrast, TGZ caused only a modest induction of apoptosis. These results were verified by histochemistry using the specific DNA stain DAPI to observe nuclear condensation, a marker of apoptosis. Finally, a brief exposure of MDA-MB-231 cells to 15dPGJ$_2$ initiated an irreversible apoptotic pathway that inhibited the growth of tumors in a nude mouse model. These findings illustrate that induction of apoptosis may be the primary biological response resulting from PPARγ activation in some breast cancer cells and further suggests a potential role for PPARγ ligands for the treatment of breast cancer.

Introduction

A common feature of tumor cells is their failure to terminally differentiate in response to appropriate stimuli. The degree of tumor cell differentiation can dictate the rate of proliferation, malignant potential and sensitivity to therapeutic interventions. Therefore, there have been major efforts to uncover novel agents and mechanisms that control tumor cell differentiation. There is extensive literature on the use of retinoic acids and their derivatives, acting through their receptors [retinoic acid receptor (RAR) and retinoid X receptor (RXR)], to arrest or reverse cancer in both animals and humans (1–10). Another member of the nuclear hormone receptor family, peroxisome proliferator-activated receptor γ (PPARγ), is preferentially expressed in adipose tissue and has an important role in fat metabolism and adipocyte differentiation (11–16). Ligands, including thiazolidinediones (TZDs) (17), certain fatty acids (18,19) and metabolites of arachidonic acid (20,21), induce activation of PPARγ and association with RXR to form a functional heterodimer (22).

Recent data reveal that PPARγ is expressed in colonic tumors and metastatic breast adenocarcinomas (23–25). The discovery of PPARγ in neoplastic cells raises the critical question of its functional significance in human cancers. Ligand activation of PPARγ inhibits proliferation and causes lipid accumulation in cultured breast cancer cells and some breast cancer cell lines (24,26). A recent study suggested that addition of the RAR agonist all-*trans*-retinoic acid (ATRA) plus a PPARγ agonist induced apoptosis of human breast cancer cells *in vitro* and attenuated tumor growth in mice (27).

In the current study we show that addition of a known prostanoid PPARγ ligand, 15-deoxy-Δ12,14-prostaglandin J_2 (15dPGJ$_2$) (23,24), inhibits the proliferation of breast cancer cells by blocking cell cycle progression (G_1 arrest) and inducing early and late events associated with apoptosis. Furthermore, pretreatment of MDA-MB-231 cells with 15dPGJ$_2$ attenuates the capacity of these cells to induce tumors in nude mice. Together, these data show that prostanoids such as 15dPGJ$_2$ may represent an important group of molecules that have the capacity to induce apoptosis of certain neoplastic cells and by this action inhibit tumorigenesis.

Materials and methods

Cells and reagents

MDA-MB-231 (28) and MCF-7 breast cancer epithelial cells were maintained in Dulbecco's modified Eagle's medium, 10% fetal calf serum (Life Technologies, Grand Island, NY), 1% penicillin and 1% streptomycin (BioWhitaker, Walkersville, MD). All prostaglandins (PGs) were purchased from Cayman Chemical (Ann Arbor, MI). Troglitazone (TGZ) was a generous gift from Parke Davis/Warner Lambert (Plainsboro, NJ).

RT–PCR analysis of PPARγ mRNA

PPARγ primers (5′-primer CCTGGCTCAGATGGCTCGG and 3′-primer CCTACGTTTAGAAGGCC) were used with total RNA isolated from MDA-MB-231 cells using the Wizard Total RNA isolation kit (Promega, Madison, WI). RT–PCR was performed using the GeneAmp RNA PCR kit and AmpliTaq Gold DNA polymerase (Perkin Elmer, Foster City, CA). Total RNA (200 ng) was converted to single-stranded cDNA and then AmpliTaq Gold (5 U) was added. Following PCR (35 cycles of 94°C for 1 min, 52°C for 30 s and 72°C for 30 s), the products were separated on a 2% agarose gel and visualized by ethidium bromide staining. Control reactions were performed in parallel in

Abbreviations: ATRA, all-*trans*-retinoic acid; DAPI, 4′,6-diamidine-2′-phenylindole diHCl; Δ12-PGJ$_2$, Δ12-prostaglandin J$_2$; 15dPGJ2, 15-deoxy-Δ12,14-prostaglandin J$_2$; PBS, phosphate-buffered saline; PPARγ, peroxisome proliferator-activated receptor γ; PG, prostaglandin; RAR, retinoic acid receptor; RXR, retinoid X receptor; TGZ, troglitazone; TZD, thiazolidinedione.

which RNA was omitted from the cDNA synthesis reaction. The cDNA band was excised from the gel and the DNA isolated using the Wizard DNA isolation kit (Promega). The DNA was sequenced and analyzed in the Core DNA Facility (Wake Forest University School of Medicine, Winston Salem, NC).

Luciferase reporter assay

MDA-MB-231 cells were seeded and allowed to grow to near confluence in 100 mm tissue culture dishes. Cells were then transiently transfected with the luciferase reporter plasmid (a generous gift from Dr Bruce Spiegleman's laboratory) and appropriate controls using Superfect (Qiagen, Valencia, CA) according to the manufacturer's protocol. Cells were then washed using phosphate-buffered saline (PBS), provided with various concentrations of 15dPGJ$_2$ and incubated for 48 h at 37°C and 5% CO$_2$. After the incubation period, cells were transfered into 15 ml conical tubes using a rubber policeman, centrifuged to pellet the cells and washed twice in PBS. The medium was removed and cells were assayed for luciferase activity using the Luciferase Activity kit (Promega) and a Turner TD-20E luminometer (Sunnyvale, CA).

Analysis of cell cycle

Cells were incubated in the presence of the indicated concentrations of PGs, including PGF$_{2\alpha}$, PGJ$_2$, Δ12-PGJ$_2$ and 15dPGJ$_2$. After an 18 h incubation, cells were pelleted and resuspended in 70% ice-cold ethanol, pelleted again and stained with propridium iodide for cell cycle analysis. Ploidy status was determined using a Coulter Epics XL-MCL flow cytometer (Hileah, FL) and percentage of cells in S phase of the cell cycle was determined using ModFit (Verity Software House Inc., Topsham, ME). In separate experiments, incubations were allowed to proceed for 48 h, cells were pelleted, resuspended and counted on a hemocytometer.

Video time-lapse microscopy

Apoptosis in neoplastic cells is characterized by specific morphological events that can be observed by video time-lapse microscopy. Previous studies have documented the specific morphological events associated with apoptosis in neoplastic cells (29–31). These specific apoptotic events begin with adherent cells becoming round (cellular rounding), followed by membrane blebbing. A proportion of cells send out echinoid-type protrusions, or spikes, followed by the cessation of movement. Finally, cells blister and expel their cytoplasmic contents into the medium. In these experiments, MDA-MB-231 cells were treated with 15dPGJ$_2$ (10 μM) or TGZ (100 μM) and placed on a Zeiss Axiovert 135 phase contrast microscope equipped with a warm stage heater/recirculator device that maintained the cell culture at 37°C temperature and 5% CO$_2$/95% air atmosphere. Cells were illuminated with red light and images were obtained using a Dage-MTI 100 CCD camera and recorded using a Panasonic AG-6740 video time-lapse recorder at a fixed rate of 1 frame/10 s (600:1 final time-lapse). The numbers of cells showing apoptotic morphology, including cellular rounding, blebbing, production of echinoid spikes, cessation of movement, blistering and cellular lysis, were assessed and the events of apoptosis were characterized and recorded for each cell in the field of view (29–31). The percentage of cells in the field of view that undergo each specific event of apoptosis was graphed as a function of time for each agonist.

Histochemical methods

Nuclear condensation and segmentation are specific events observed during apoptosis (32–34). As an additional marker, nuclear morphology was examined using histochemical staining with 4′,6-diamidine-2′-phenylindole diHCl (DAPI) (Sigma, St Louis, MO), a fluorescent dye that selectively labels DNA. Briefly, 1.0×10^6 MDA-MB-231 cells were incubated with 15dPGJ$_2$ (10 μM) or TGZ (100 μM) in 35 mm culture dishes. After a 36 h incubation, suspended cells contained in the medium were centrifuged onto a glass slide using a Cytospin 3. Both adherent cells in culture dishes and suspended cells centrifuged onto slides were then fixed in 10% v/v formalin in PBS (15 min, 23°C). This was followed by incubation with 0.1 μg/ml DAPI in methanol (15 min, 23°C). After washing, cells were mounted under a coverslip in glycerol and viewed using a Zeiss Axioplan-2 epifluorescence microscope equipped with UV excitation filters. Digital images of suspended and adherent cells were recorded using a Spot camera.

Tumor growth in nude mice

Three-week-old female BALB/C nude mice were purchased from Charles River (Raleigh, NC) and housed in the Animal Care Facility (Wake Forest University School of Medicine, Winston Salem, NC). The nude mouse model for the study of invasion and metastasis of tumors *in vivo* (28,35) was used to determine the progression of MDA-MB-231 cells after treatment with PPARγ agonists. Briefly, MDA-MB-231 cells were incubated with 15dPGJ$_2$ (10 μM) for 18 h and viability was determined by trypan blue exclusion. Viable cells (7.5×10^5) in 100 μl culture medium were transplanted by s.c. injection into the right breast pad and viable vehicle-treated cells (7.5×10^5) in 100 μl culture medium were transplanted by s.c. injection into the left
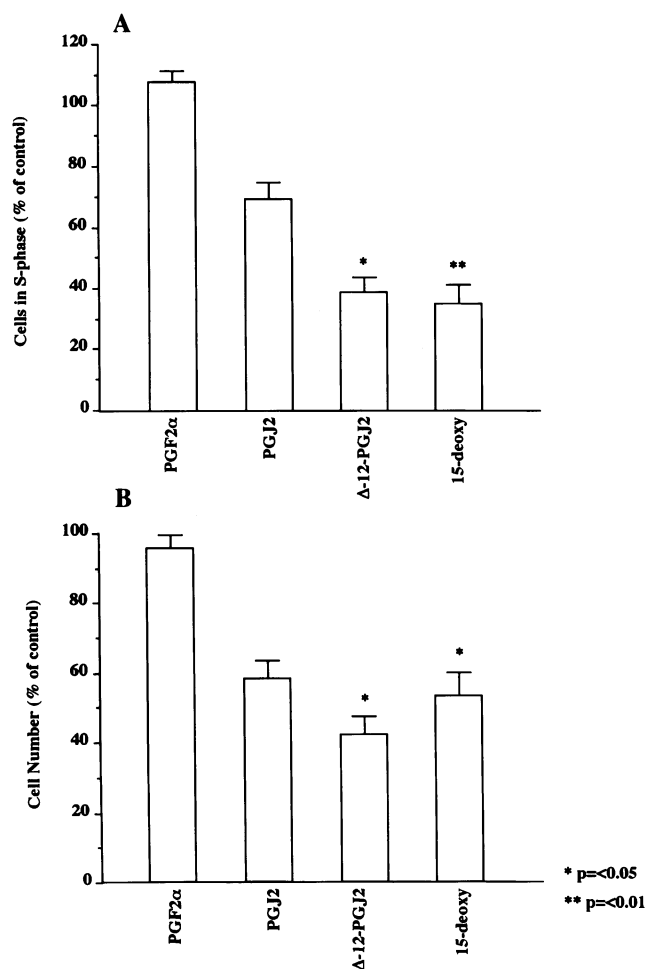
Fig. 1. Influence of PGs on breast cancer cell growth. Total cell number and the percentage of cells traversing the S-phase of the cell cycle was observed as markers of cell cycle progression in MDA-MB-231 breast cancer cells after the addition of the exogenous prostaglandins PGJ$_2$, its metabolites Δ12-PGJ$_2$ and 15dPGJ$_2$ and PGF$_{2\alpha}$. MDA-MB-231 cells (1.0×10^6) were incubated with 10 μM of the various PGs for 18 (**A**) or 48 h (**B**) for analysis of cellular proliferation. Percentage of cells in S phase was determined by flow cytometry and total cell number was assessed using a Coulter cell counter. Data are representative of means ± SEM of four separate experiments.

breast pad of mice. Tumor area was measured every third day beginning 7 days post-injection.

Results

Expression of PPARγ and cellular proliferation

Initial studies investigated the expression of PPARγ mRNA in the estrogen receptor-negative breast cancer cell line MDA-MB-231. RT–PCR analysis readily detected the PPARγ mRNA in MDA-MB-231 breast cancer cells (data not shown). DNA sequencing confirmed that the expected sized PCR product (1002 bp) was identical to the human PPARγ cDNA sequence.

To determine the effect of PGs on cell proliferation, MDA-MB-231 cells were incubated with 10 μM PGF$_{2\alpha}$, PGJ$_2$, Δ12-prostaglandin J$_2$ (Δ12-PGJ$_2$) or 15dPGJ$_2$ and total cell number as well as the capacity of cells to move into S phase of the cell cycle was determined as a measure of cell proliferation. The number of cells traversing the S phase of the cell cycle (Figure 1A) was markedly reduced after 18 h of exposure to a known PPARγ agonist, 15dPGJ$_2$ (20,21). In contrast, a PG that does not bind PPARγ, PGF$_{2\alpha}$ (18–21), did not influence
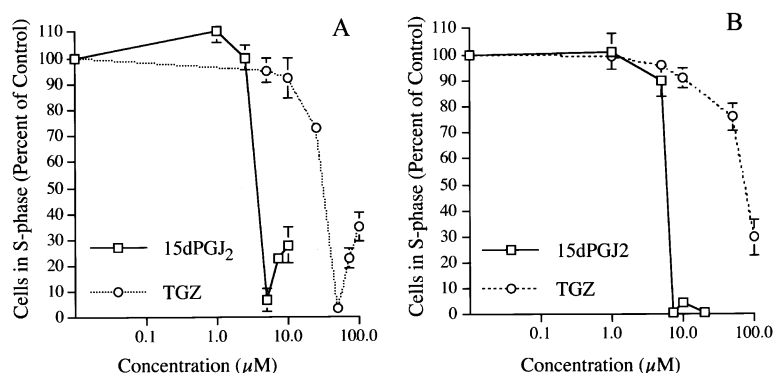
Fig. 2. Dose-dependent response of PPARγ agonists on cell cycle progression in MDA-MB-231 and MCF-7 cells. MCF-7 (**A**) and MDA-MB-231 (**B**) cells (1.0×10^6) were incubated for 18 h with 15dPGJ$_2$ at concentrations ranging from 0.1 to 20 µM or with TGZ at concentrations ranging from 0.1 to 100 µM for 18 h. The percentage of cells in S phase was determined by flow cytometry. Data are representative of means ± SEM of three separate experiments.

either marker of cellular proliferation. Total cell number was also determined after incubation with the test compounds for 48 h (Figure 1B). Cell number was significantly decreased by the PGJ$_2$ metabolites Δ12-PGJ$_2$ and 15dPGJ$_2$. Together, these data reveal that MDA-MB-231 breast cancer cells express mRNA encoding PPARγ and that PGs of the J series reduce the proliferation of these cells.

The next experiments investigated the dose–response relationship of two known PPARγ agonists on cellular proliferation (Figure 2). Estrogen receptor-negative MDA-MB-231 and estrogen receptor-positive MCF-7 cells were incubated with 15dPGJ$_2$ (0.1–20 µM) or TGZ (0.1–100 µM) for 18 h and the percentage of cells in the S phase of the cell cycle was determined by flow cytometry. Exposure of both cell lines to high concentrations of either PPARγ agonist blocked cell cycle progression. However, the prostanoid agonist 15dPGJ$_2$ inhibited cell cycle at concentrations 10-fold lower than TGZ in the MDA-MB-231 cell line. 15dPGJ$_2$ was a potent inhibitor of the cell cycle in MCF-7 cells and TGZ was a more potent inhibitor of the cell cycle in MCF-7 than in MDA-MB-231 cells.

In order to test the transcriptional activation of PPARγ by 15dPGJ$_2$ we performed luciferase reporter assays by transient transfection of MDA-MB-231 cells with a plasmid containing the PPARγ response element upstream of the luciferase reporter construct. Increasing concentrations of 15dPGJ$_2$ resulted in a dose-dependent increase in luciferase activity (Table I). These results suggest that 15dPGJ$_2$ induces cell cycle inhibition by direct interaction with PPARγ.

Influence of 15-deoxy-Δ12,14-PGJ$_2$ on differentiation and apoptosis

Several investigators have demonstrated that PPARγ agonists can induce differentiation in neoplastic cells, including breast adenocarcinoma and liposarcoma cells (23–26). A hallmark of cellular differentiation is the accumulation of intracellular neutral lipid which can be stained with the fluorescent lipophilic stains Nile Red or Oil Red O and easily visualized by fluorescent microscopy (36–38). Thus, we used these stains in the next experiments and examined whether addition of 15dPGJ$_2$ to MDA-MB-231 cells also induces differentiation. Unlike the reported action of TZDs, which increase lipid accumulation in breast cancer cells (24,26), treatment of MDA-MB-231 cells with 15dPGJ$_2$ (10 µM) for 24, 48 or 96 h had no significant effect on accumulation of cellular lipid (data not shown). However, treatment of MDA-MB-231 cells with

**Table I.** Luciferase reporter activity of MDA-MB-231 cells exposed to various concentrations of 15dPGJ$_2$

Vector	15dPGJ$_2$ (µM)	Relative light intensity
Negative control	0.0	0.00
Positive control	0.0	363.00
DR-1 vector	0.0	0.78
DR-1 vector	2.5	2.94
DR-1 vector	5.0	11.50
DR-1 vector	10.0	73.20
DR-1 vector	20.0	9255.00

MDA-MB-231 cells were transiently transfected with the PPARγ response element upstream of a luciferase reporter construct (DR-1 vector) (Materials and methods). A vector containing a CMV promoter but no gene was used as a negative control and a luciferase construct driven by the CMV promoter was used as a positive control. Cells were provided with the indicated concentrations of 15dPGJ$_2$ for 48 h and then assayed for luciferase activity. Data are reported as relative light intensity units and are representative of three separate experiments.

15dPGJ$_2$ (10 µM) was associated with a consistent decrease in cell viability and proliferation. This finding raised the question of whether 15dPGJ$_2$ may induce signaling events that lead to the induction of apoptosis.

Chromatin condensation is an early event of apoptosis (29–34). MDA-MB-231 cells treated with 15dPGJ$_2$ (10 µM) or TGZ (100 µM) for 36 h show a marked increase in nuclear condensation, as indicated by the dense staining pattern of DAPI. 15dPGJ$_2$- and TGZ-treated cells that remained attached to the cell culture dish show the characteristic staining morphology of apoptotic cells (Figure 3). In addition, cells that were suspended in medium also underwent apoptosis (Figure 4). The changes in cell surface morphology of 15dPGJ$_2$-treated cells was viewed by phase contrast (Figures 3C and 4C) and nuclear condensation of the same cell population was viewed by UV excitation (Figures 3C′ and 4C′). TGZ-treated cells also showed nuclear changes associated with apoptosis as seen by phase contrast microscopy (Figures 3B and 4B) and by UV excitation (Figures 3B′ and 4B′). Arrows indicate cell nuclei that are in the process of apoptosis. In contrast, control cells did not undergo apoptosis (Figures 3A and A′ and 4A and A′). Rather, two cells can be seen in the early stages of mitosis and anaphase of mitosis as indicated by arrowheads (Figure 4A′). These data reveal that agonists of PPARγ can induce apoptosis in MDA-MB-231 cells.

In addition to DNA condensation and segmentation during
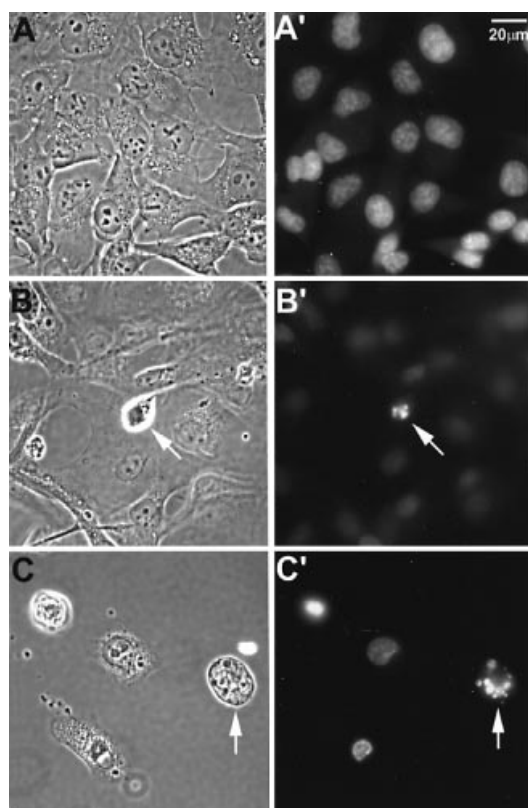
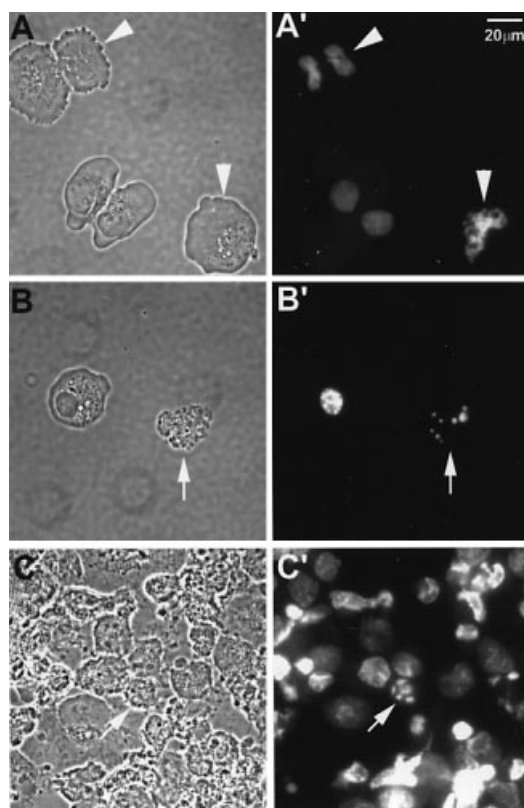**Fig. 3.** Nuclear changes associated with exposure of MDA-MB-231 cells to 15dPGJ$_2$ or TGZ. MDA-MB-231 cells (1.0×10^6) were treated with vehicle alone (**A**), 100 μM TGZ (**B**) or 10 μM 15dPGJ$_2$ (**C**) for 36 h. Medium was collected and cells which remained attached to the cell culture dish were fixed with 10% v/v formamide and stained with DAPI (0.1 μg/ml). Nuclear morphology was examined as described in Materials and Methods. Arrows indicate apoptotic cells. These data are representative of three separate experiments.

Fig. 4. Nuclear changes associated with exposure of MDA-MB-231 cells to 15dPGJ$_2$ or TGZ. MDA-MB-231 cells (1.0×10^6) were treated with vehicle alone (**A**), 100 μM TGZ (**B**) or 10 μM 15dPGJ$_2$ (**C**) for 36 h. Medium was collected and cells, which were suspended in culture medium, were centrifuged onto a glass slide. Cells were then fixed with 10% v/v formamide and stained with DAPI (0.1 μg/ml). Nuclear morphology was examined as described in Materials and methods. Arrows indicate apoptotic cells and arrowheads indicate cells in mitosis. These data are representative of three separate experiments.

apoptosis, specific changes in cell surface morphology can be recorded by video time-lapse microscopy. The morphological changes associated with the progression of apoptosis include initial cell rounding, surface membrane blebbing, cessation of movement and extension of echinoid spikes followed by membrane blistering and lysis (29–31). Video time-lapse microscopy was used to record these events in MDA-MB-231 cells exposed 15dPGJ$_2$ or TGZ (Figure 5). Treatment of MDA-MB-231 cells with 15dPGJ$_2$ (10 μM) induced all of the characteristic morphological changes associated with apoptosis (Figure 5A). Cellular rounding and membrane blebbing, the earliest features of apoptosis, were observed from 8 to 30 h after treatment, but cells remained attached to the culture dish and were still viable by trypan blue exclusion. Cells ceased movement and produced echinoid spikes beginning at 20 h post-treatment. By 48 h >60% of cells had undergone blistering and lysis, the last events of apoptosis. Treatment of MDA-MB-231 cells with TGZ (100 μM) induced a slower and more modest response (Figure 5B). Only 30% of cells had completed apoptosis by 50 h. In contrast, treatment of MDA-MB-231 cells with vehicle alone did not induce any of the events of apoptosis. Rather, all of the cells in this group underwent at least one mitosis and the cell population doubled after 24 h.

In vivo inhibition of tumorigensis

The next experiments were designed to determine whether a brief *in vitro* exposure of breast cancer cells to 15dPGJ$_2$ could influence the capacity of these cells to generate tumors in nude

mice. MDA-MB-231 cells were treated for 18 h with 15dPGJ$_2$ (10 μM) and 7.5×10^5 viable cells were transplanted by s.c. injection into the right breast pad and 7.5×10^5 control cells were transplanted by s.c. injection into the left breast pad of 3-week-old female nude mice (Figure 6). Untreated control cells rapidly developed visible tumors and dramatic growth was observed throughout the time course. In contrast, a one time treatment of cells with 15dPGJ$_2$ markedly attenuated their capacity to develop visible tumors. Moreover, these tumors grew to a significantly smaller size compared with untreated control tumors.

Discussion

In this study we have demonstrated that MDA-MB-231 cells express PPARγ mRNA and that treatment of MDA-MB-231 and MCF-7 cells with the PPARγ agonists 15dPGJ$_2$ and TGZ reduces their proliferative capacity. Furthermore, 15dPGJ$_2$ and TGZ induce morphological changes in MDA-MB-231 cells that are associated with the onset and progression of apoptosis. 15dPGJ$_2$ is associated with strong transcriptional activation of a PPARγ response element in a reporter gene assay system. Finally, brief exposure of MDA-MB-231 cells to 15dPGJ$_2$ markedly attenuated tumor formation in a nude mouse model. Together, these results suggest that apoptosis, not differentiation, is the primary biological response for PPARγ activation by 15dPGJ$_2$ in some breast cancer cell lines.
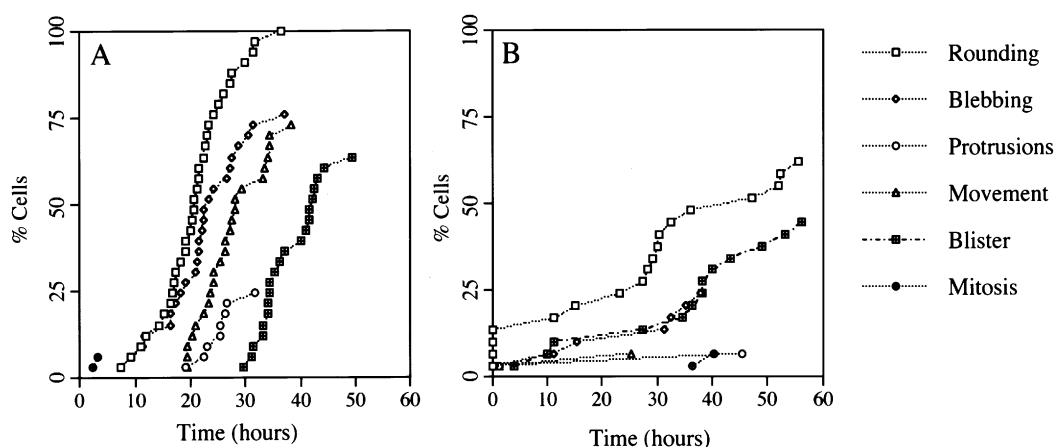
Fig. 5. Video time-lapse microscopy of MDA-MB-231 cells treated with 15dPGJ$_2$ or TGZ. MDA-MB-231 cells (1.0×10^6) were treated with 10 μM 15dPGJ$_2$ (**A**) or 100 μM TGZ (**B**) and images were recorded using a video time-lapse recorder at the rate of 1 frame/10 s (final time lapse equals 600:1). Each cell in the field of view was followed from the time of seeding to the indicated stop time. The events associated with apoptosis or mitosis for each cell were recorded from the time of seeding. These data are representative of three separate experiments.

Many developing anticancer therapies focus on two cellular pathways, differentiation and apoptosis. Differentiation agents, such as retinoids, have been used in many types of cancer and have proven clinical utility in leukemia and Kaposi's sarcoma (1–10). Like retinoids, agonists of PPARγ induce formation of a functional heterodimer with RXR (22). Moreover, activation of PPARγ in liposarcoma cells has been shown to induce differentiation (11–16), indicating that PPARγ activation may be a promising therapeutic approach for cancers of mesenchymal cell origin. It is not clear, however, how PPARγ activation affects cell growth in cancers of endodermal origin. Treatment of several breast cancer cell lines (21MT, MCF-7, T47D, MDA-MB-231 and BT474), infiltrating primary intraductal carcinoma and normal murine breast epithelial cells with the PPARγ agonist TZD drugs has been shown to inhibit cell growth in some cases and induce events associated with terminal differentiation (15,23,24,26). Our data reveal that treatment of MDA-MB-231 cells with the PPARγ ligand 15dPGJ$_2$ inhibits cell proliferation by blocking entry into the S phase of the cell cycle. Furthermore, this block is not associated with differentiation, but apoptosis. Based on video time-lapse microscopy, this process requires 36–48 h to complete. Recently, Elstner *et al.* (27) demonstrated apoptosis of MCF-7 cells treated with PPARγ agonists, but only after the addition of both ATRA and 15dPGJ$_2$ or TGZ for 96 h.

By incorporating the technology of video time-lapse microscopy, we have been able to follow the events of apoptosis from onset to completion. These events include cellular rounding, blebbing, the production of echinoid protrusions and blistering, followed by cell lysis, but did not include the formation of DNA ladders, as is traditionally seen by gel electrophoresis. Collins *et al.* (30) have shown that DNA ladder formation is a very late event in some cells that follows the events we have documented by video time-lapse microscopy. This technology allows for a more precise examination of events that occur after exposure of breast cancer cells to PPARγ agonists. Early nuclear condensation followed by surface morphological changes in response to 15dPGJ$_2$ support the contention that MDA-MB-231 cells undergo many of the classical events associated with the onset and progression of apoptosis. Furthermore, similar to findings that have been reported for 21PT breast cancer cells (24), once these cells had been exposed to a PPARγ agonist, removal of the agonist did not result in a
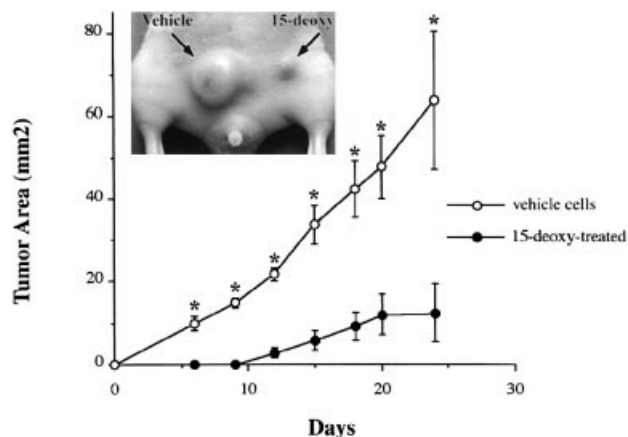
Fig. 6. Tumor progression in nude mice. MDA-MB-231 cells were treated with 10 μM 15dPGJ$_2$ for 18 h. Control treatment consisted of vehicle without drug. Viable control-treated cells (7.5×10^5) were injected s.c. into the right breast pad and viable 15dPGJ$_2$-treated cells (7.5×10^5) were injected s.c. into the left breast pad of female nude mice. Tumor area (mm^2) was determined every 3 days after the onset of visible tumor growth. Open circles represent vehicle-treated cells and closed circles represent 15dPGJ$_2$-treated cells. These data represent the mean areas $\pm$ SEM of three separate experiments ($n = 7$ mice/experiment).

renewed capacity for growth and tumorigenesis *in vivo*. This suggests that brief activation of PPARγ by 15dPGJ$_2$ may be sufficient to stimulate an irreversible apoptotic pathway.

It is interesting to note that TGZ was a less potent inducer of apoptosis in our studies than 15dPGJ$_2$. The reasons for these differences have yet to be uncovered. One explanation may be that a novel receptor for endogenous J series PGs may be involved in the signal transduction events that lead to apoptosis in these cells, similar to the adenylyl cyclase-coupled PGE$_2$ and PGF$_1$ receptors which have been described in liver cells (45). However, PPARγ reporter assays and published data suggest a strong correlation between 15dPGJ$_2$ and PPARγ activation (18–21,24,27). Secondly, the fact that 15dPGJ$_2$ has been used sparingly in many of the previous studies of neoplastic cells may explain why a strong correlation between PPARγ activation and apoptosis has not yet been made. Thirdly, because 15dPGJ$_2$ is a potent PPARγ agonist, the high degree of PPARγ activation observed in this study may be higher than that which has been reported using TZDs in other studies. To

our knowledge this is the first neoplastic cellular system where activation of PPARγ alone is associated with apoptosis.

It is becoming clear that activation of the same receptor with different ligands may result in different responses. Differentiation is the dominant biological response to activation of PPARγ with TZDs in liposarcoma cells, whereas in our studies with breast cancer cell lines, 15dPGJ$_2$ induces apoptosis. In colonic tumors, PPARγ activation with synthetic ligands has shown both an increase in colon polyp formation and a reversal of malignant changes (39–41) under different experimental conditions. In activated monocytes and macrophages, PPARγ activation with natural agonists inhibits the production of inflammatory cytokines and the expression of inducible nitric oxide synthase (42,43) that may be key events in the induction of apoptosis in human macrophages (44). Clearly, the molecular mechanisms that lead to these differing results must be elucidated to facilitate more rational approaches for the treatment of different cancers that express PPARγ. The current study reveals the potential to utilize prostaglandin agonists of PPARγ for the treatment of breast cancers that express PPARγ and the exciting possibility that these compounds may induce apoptotic cell death.

Acknowledgements

References

1. Heyman,R.A., Mangelsdorf,D.J., Dyck,J.A., Stein,R.B., Eichele,G., Evans, R.M. and Thaller,C. (1992) 9-*cis* retinoic acid is a high affinity ligand for the retinoid X receptor. *Cell*, **68**, 397–406.
2. Levin,A.A., Sturzenburger,U., Kazmer,S. *et al.* (1992) 9-*cis* retinoic acid stereoisomer binds and activates the nuclear receptor RXR alpha. *Nature*, **23**, 359–361.
3. Moon,R.C. Mehta,R.G. and Rao,K.V.N. (1994) Retinoids and cancer in experimental animals. In Sporn,M.B., Roberts,A.B. and Goodman,D.S. (eds) *The Retinoids: Biology, Chemistry and Medicine*, 2nd Edn. Raven Press, New York, NY, pp. 573–595.
4. Marth,R.C., Mayer,I. and Daxenbichler,G. (1984) Effect of retinoic acid and 4-hydroxytamoxifen on human breast cancer cell lines. *Biochem. Pharmacol.*, **33**, 2217–2221.
5. Fontana,J.A., Miranda,D. and Mezu,A.B. (1990) Retinoic acid inhibition of human breast carcinoma proliferation is accompanied by inhibition of the synthesis of a Mr 39,000 protein. *Cancer Res.*, **50**, 1977–1982.
6. van der Burg,B., van der Leede,B.M., Kwakkenbos-Isbrucker,L., Salverda,S., de Lat,S.W. and van der Saag,P.T. (1993) Retinoic acid resistance of estradiol-independent breast cancer cells coincides with diminished retinoic acid receptor function. *Mol. Cell. Endocrinol.*, **91**, 149–157.
7. Dawson,M.I., Chao,W., Pine,P. *et al.* (1995) Correlation of retinoid binding affinity to retinoic acid receptor alpha with retinoid inhibition of growth of estrogen receptor-positive MCF-7 mammary carcinoma cells. *Cancer Res.*, **55**, 4446–4451.
8. Elstner,E., Linker-Israeli,M., Umiel,T. *et al.* (1997) Combination of a potent 20-epi-vitamin D3 analogue (KH1060) with 9-*cis*-retinoic acid irreversibly inhibits clonal growth, decreases bcl-2 expression, and induces apoptosis in HL-60 leukemic cells. *Cancer Res.*, **56**, 3570–3576.
9. Elstner,E., Linker-Israeli,M., Le,J., Umiel,T., Michl,P., Said,J.W., Binderup,L., Reed,J.C. and Koeffler,H.P. (1997) Synergistic decrease of clonal proliferation, induction of differentiation, and apoptosis of acute promyelocytic leukemia cells after combined treatment with novel 20-epi vitamin D3 analogs and 9-*cis* retinoic acid. *J. Clin. Invest.*, **99**, 349–360.
10. Toma,S., Isnard,L., Raffo,P., Dastoli,G., DeFrancisi,E., Riccardi,L., Palumbo,R. and Bollag,W. (1996) Effects of all-*trans*-retinoic acid and 13-*cis*-retinoic acid on breast cancer cell lines: growth inhibition and apoptosis induction. *Int. J. Cancer*, **70**, 619–627.
11. Chwala,A., Schwartz,E.J., Dimaculangan,D.D. and Lazar,M.A. (1994)
12. Tontonoz,P., Hu,E., Graves,R.A., Budavari,A.I., and Spiegelman,B.M. (1994) mPPAR gamma2: tissue specific regulator of an adipocyte enhancer. *Genes Dev.*, **8**, 1224–1234.
13. Tontonoz,P., Hu,E. and Spiegelman,B.M. (1994) Stimulation of adipogenesis in fibroblasts by PPARγ2, a ligand-activated transcription factor. *Cell*, **79**, 1147–1156.
14. Lambe,K.G. and Tugwood,J.D. (1996) A human peroxisome-proliferator-activated receptor-gamma is activated by inducers of adipogenesis, including thiazolidinedione drugs. *Eur. J. Biochem.*, **239**, 1–7.
15. Tontonoz,P., Singer,S., Forman,B.M. *et al.* (1997) Terminal differentiation of human liposarcoma cells induced by ligands for peroxisome proliferator-activated receptor gamma and the retinoid X receptor. *Proc. Natl Acad. Sci. USA*, **94**, 237–241.
16. Hu,E., Tontonoz,P. and Spiegelman,B.M. (1995) Transdifferentiation of myoblasts by the adipogenic transcription factors PPAR gamma and C/EBP alpha. *Proc. Natl Acad. Sci. USA*, **92**, 9856–9860.
17. Lehman,J.M., Moore,L.B., Smith-Oliver,T.A., Wilison,W.O., Willson,T.M. and Kliewer,S.A. (1995) An antidiabetic thiazolidinedione is a high affinity ligand for peroxisome proliferator-activated receptor γ (PPARγ). *J. Biol. Chem.*, **270**, 12953–12956.
18. Kliewer,S.A., Sundseth,S.S., Jones,S.A. *et al.* (1997) Fatty acids and eicosanoids regulate gene expression through direct interaction with peroxisome proliferator-activated receptors α and γ. *Proc. Natl Acad. Sci. USA*, **94**, 4318–4323.
19. Yu,K., Bayona,W., Kallen,C.B., Harding,H.P., Ravera,C.P., McMahon,G., Brown,M. and Lazar,M.A. (1995) Differential activation of peroxisome proliferator activated receptors by eicosanoids. *J. Biol. Chem.*, **270**, 23975–23983.
20. Forman,B.M., Tontonoz,P., Chen,J., Brun,R.P., Spiegelman,B.M. and Evans,R.M. (1995) 15-deoxy-Δ12,14 prostaglandin J2 is a ligand for the adipocyte determination factor PPARγ. *Cell*, **83**, 803–812.
21. Kliewer,S.A., Lenhard,J.M., Wilson,T.M., Patel,I., Morris,D.C. and Lehmann,J.M. (1995) A prostaglandin J2 metabolite binds peroxisome proliferator-activated receptor γ and promotes adipocyte differentiation. *Cell*, **83**, 813–819.
22. Kliewer,S.A., Umesono,K., Noonan,D.J., Heyman,R.A. and Evans,R.M. (1992) Convergence of 9-*cis* retinoic acid and peroxisome proliferator signaling pathways through heterodimer formation of their receptors. *Nature*, **358**, 771–774.
23. Kilgore,M.W., Tate,P.L., Rai,S., Sengoku,E. and Price,T.M. (1997) MCF-7 and T47D human breast cancer cells contain a functional peroxisomal response. *Mol. Cell. Endocrinol.*, **129**, 229–235.
24. Mueller,E., Sarraf,P., Tontonoz,P., Evans, R.M., Martin,K.J., Zhang,M., Fletcher,C. and Spiegelman,B.M. (1998) Terminal differentiation of human breast cancer through PPARγ. *Mol. Cell*, **1**, 465–470.
25. DuBois,R.N., Gupta,R., Brockman,J., Reddy,B.S., Krakow,S.L. and Lazar,M.A. (1998) The nuclear eicosanoid receptor, PPARγ is abberantly expressed in colonic tumors. *Carcinogenesis*, **19**, 49–53.
26. Altiok,S., Xu,M. and Spiegelman,B.M. (1997) PPARγ induces cell cycle withdrawal: inhibition of E2F/DP DNA-binding activity via down-regulation of PP2A. *Genes Dev.*, **11**, 1987–1998.
27. Elstner,E., Mueller,C., Koshizuka,K., Williamson,E.A., Park,D., Asou,H., Shintaku,P., Said,J.W., Heber,D. and Koeffler,H.P. (1998) Ligands for peroxisome proliferator-activated receptor and retinoic acid receptor inhibit growth and induce apoptosis of human breast cancer cells *in vitro* and in BNX mice. *Proc. Natl Acad. Sci. USA*, **95**, 8806–8811.
28. Brunner,N., Thompson,E.W., Spang-Thomsen,M., Rygaard,J., Dano,K. and Zwiebel,J.A. (1992) LacZ transduced human breast cancer xenografts as an *in vivo* model for the study of invasion and metastasis. *Eur. J. Cancer*, **28A**, 1989–1995.
29. Pulkkinen,J.O., Elomaa,L., Joensuu,H., Martikainen,P., Servomaa,K. and Grenman,P. (1996) Paclitaxel-induced apoptotic changes followed by time-lapse video microscopy in cell lines established from head and neck cancer. *J. Cancer. Res. Oncol.*, **122**, 214–218.
30. Collins,J.A., Schandl,C.A., Young,K.K., Vesely,J. and Willingham,M.C. (1997) Major DNA fragmentation is a late event in apoptosis. *J. Histochem. Cytochem.*, **45**, 923–934.
31. Guo,M., Chen,C., Vidair,C., Marino,S., Dewey,W.C. and Ling,C.C. (1997) Characterization of radiation-induced apoptosis in rodent cell lines. *Radiat. Res.*, **147**, 295–303.
32. Wyllie,A.H., Beattie,G.J. and Hargreaves,A.D. (1981) Chromatin changes in apoptosis. *Histochem. J.*, **13**, 681–692.
33. Walker,N.I., Harmon,B.V., Gobe,G.C. and Kerr,J.F. (1988) Patterns of cell death. *Methods. Achiev. Exp. Pathol.*, **13**, 18–54.

34. Compton,M.M. (1992) A biochemical hallmark of apoptosis: inter-nucleosomal degredation of the genome. *Cancer Metastasis Rev.*, **11**, 105–119.

35. Brunner,N., Boysen,B., Romer,J. and Spang-Thomsen,M. (1993) The nude mouse model as an *in vivo* model for human breast cancer invasion and metastasis. *Breast Cancer Res. Treat.*, **24**, 257–264.

36. Fowler,S.D. and Greenspan,P. (1985) Application of Nile red, a fluorescent hydrophobic probe, for the detection of neutral lipid deposits in tissue sections: comparison with oil red O. *J. Histochem. Cytochem.*, **33**, 833–836.

37. Greenspan,P., Mayer,E.P. and Fowler,S.D. (1985) Nile red: a selective fluorescent stain for intracellular lipid droplets. *J. Cell Biol.*, **100**, 965–973.

38. Kute,T.E., Shao,Z.M., Sugg,N.K., Long,R.T., Russel,G.B. and Case,L.D. (1992) Cathepsin D and other markers as prognostic indicators for node negative breast cancer patients. *Cancer Res.*, **52**, 5198–5203.

39. Sarraf,P., Mueller,E., Jones,D. *et al.* (1998) Diferentiation and reversal of malignant changes in colon cancer through PPARgamma. *Nature Med.*, **4**, 1046–1052.

40. Lefebvre,A.M., Chen,I., Desreumaux,P., Najib,J., Fruchart,J.C., Geboes,K., Briggs,M., Heyman,R. and Auwerx,J. (1998) Activation of the peroxisome proliferator-activated receptor gamma promotes the development of colon tumors in C57BL/6J-APC/+ mice. *Nature Med.*, **4**, 1053–1057.

41. Saez,E., Tontonoz,P., Nelson,M.C., Alvarez,J.G., Ming,U.T., Barid,S.M., Thomazy,V.A and Evans,R.M. (1998) Activators of the nuclear receptor PPARgamma enhance polyp formation. *Nature Med.*, **4**, 1058–1061.

42. Ricote,M., Li,A.C., Willson,T.M., Kelly,C.J and Glass,C.K. (1998) The peroxisome proliferator-activated receptor-γ is a negative regulator of macrophage activation. *Nature*, **39**, 79–82.

43. Jiang,C., Ting,A.T. and Seed,B. (1998) PPAR-γ agonists inhibit production of monocyte inflammatory cytokines. *Nature*, **39**, 82–86.

44. Chinetti,G., Griglio,S., Antonucci,M., Torra,I.P., Delerive,P., Majd,Z., Fruchart,J.C., Chapman,J., Najib,J. and Staels,B. (1998) Activation of proliferator-activated receptors α and γ induces apoptosis of human monocyte-derived macrophages. *J. Biol. Chem.*, **273**, 25573–25580.

45. Okamura,N. and Terayama,H. (1977) Prostaglandin receptor–adenylate cyclase system in plasma membranes of rat liver and ascites hepatomas, and the effect of GTP upon it. *Biochim. Biophys. Acta*, **465**, 54–67.